

# Feeding behaviour of graphite containing material

HEINZ-JOSEF WOJTAS

Fakultät für Ingenieurwissenschaften, Institut für Angewandte Materialtechnik,  
Universität Duisburg-Essen, Lotharstr. 65, D-47057 Duisburg;  
E-mail: hk225wo@uni-duisburg.de

Received: June 30, 2005    Accepted: November 24, 2005

**Abstract:** On casting and cooling of metals in a mould energy in form of heat will be transferred from the liquid metal to the moulding material. The mechanism of energy transfer and the corresponding capture capacity of the moulding material define the energy transfer in form of heat by cooling of the metal at contemporaneous heating of the moulding material. Only the exact knowledge of the temporary and quantitative process of heat flow will lead a solidification simulation to correct results. According to second law of thermodynamics energy in the form of heat may only be transferred from a colder to a warmer material if this is forced by mechanical work. Self-transfer of heat is only possible from an area of higher temperature in direction to areas with lower temperature. Only on the premises of a temperature drop a self-transfer of heat is possible. The energy transfer between materials of different temperatures is finished when an energetic balance is reached, i.e. when after the heat transfer there is the same temperature at all materials. Energy in the form of heat is transferred by means of heat conductivity, heat transfer (heat convection) or heat radiation.

**Key words:** metal/mould material, graphite, heat transfer, conductivity, energy balance, feeding

## PART 1: DEFINITION OF VARIOUS INFLUENCING VARIABLES

### PHYSICAL VALUES DEFINING THE SOLIDIFICATION PROCESS

#### Density ( $\rho$ )

The density of a substance is the relation of mass to volume, some times called “specific mass”. Although most of the solid bodies and liquids expand on heating, these volume changes are relatively small and nearly independent of temperature and pressure.

#### Thermal conductivity ( $\lambda$ )

Thermal conductivity means the energy transport inside a substance by interaction of atoms and molecules, which are not transported themselves (for example within the single silica grain, the solidified crystal or the convection-free melt). The energy transport is done in the way, that quicker and larger swinging molecules of a more heated substance area continue to transfer energy to adjoining and less heated substance regions, until – after energy transfer is

finished – the same average swinging condition and the same temperature is set.

Thermal conductivity of various materials is different. It is expressed by thermal conductivity  $\lambda$ . Thermal conductivity of different materials is experimentally investigated and depends on temperature.

### **Heat transfer (sometimes called “heat convection”)**

Under the term “heat transfer” is to be understood an energy transport between several materials (for example between two touching silicate grains or the solidified casting surface and the mould material) with different temperature and without material transport. Energy transfer is done in the touching area of both substances and implies a temperature drop. After heat transfer is finished both substances have the same temperature  $T$  within the touching area.

Real heat convection is combined with a material transfer. This materials transfer is called forth within liquid and gaseous materials by a thermal change of volumes and density. Heat convection within liquid metals is detectable only at an early stage of mould filling. Heat convection of air has not been detected within a mould. The pressure build-up within pore volume of the mould by means of evaporation or combustion processes does not belong to the physical values, but to the variable moulding material values defining the solidification process.

### **Heat transition**

If liquids or gases of different temperatures are separated by a solid wall, an energy

transfer will take place, consisting of heat conduction and heat transfer. This combined form of heat transfer is called heat transition.

### **Heat radiation**

Between bodies of different temperatures heat is not only transferred by means of thermal conductivity or heat convection but also at same time by means of heat radiation (for example across the gap between the silicate grains). Everywhere at heat transfer processes the kinetic energy of the molecules is partially transferred into radiation energy and radiated. The percentage of radiation energy at complete energy transfer is small at low temperatures.

Heat radiation belongs to electro-magnetic waves and they are within visible frequency range only at higher temperatures. Frequency range, diffusion, reflection and refraction follow the valid regularities of luminous radiation.

The radiation energy impacting a radiated body may be absorbed reflected or transmitted. The absorbed part of the radiation energy will be transferred again into kinetic energy of the molecules and will heat the radiated body which therefore becomes source of own radiation.

A body absorbing all impacting radiation energy is called an absolute black body. Absorption and emission are on highest level.

The heat  $Q$  radiated from an absolute black body with a surface  $A$  within a time  $t$  depends on the body temperature  $T$  and results from the law of Stefan Boltzmann.

### Amount of heat

The amount of heat  $Q$  is the quantity of energy in the form of heat, which can be feed to a material or taken away. On thermo-technical calculation there is often a reference to material quantity of 1 kg. The amount of heat referring to 1 kg is called specific heat  $q$ .

### Specific heat capacity ( $c_p$ )

The specific heat capacity ( $c_p$ ) characterizes the various heating-up of materials. It indicates the amount of energy in the form of heat, which is necessary to heat a material quantity with a mass of 1 kg for 1 K (or 1°C) by keeping the respective aggregate state. If a material quantity with the mass  $m_1$  and the temperature  $T_1$  shall be heated to a temperature  $T_2$  by supply of heat this adding heat results of:

$$Q = mc_p (T_2 - T_1) \quad (1)$$

Those materials that extend noticeable during heating is to differ between heat capacities at constant pressure and constant volume respectively. This is irrelevant for liquids and solid bodies due to the unimportant volume modification. Although it is normally calculated with heat capacity at constant pressure.

### VARIABLE MOULDING MATERIAL

#### VALUES DEFINING THE SOLIDIFICATION PROCESS

#### Density, bulk density, packing density ( $\rho$ )

At production of moulds a loose, granular material conglomerate is compacted on machines. The voids fraction between the grains decreases. Generally you have to assume considerable density fluctuation for all moulds. The density fluctuation varies with type and sort of sand, binder, moulding box and method of compacting. By this the voids fraction fluctuates, too, and – as a result

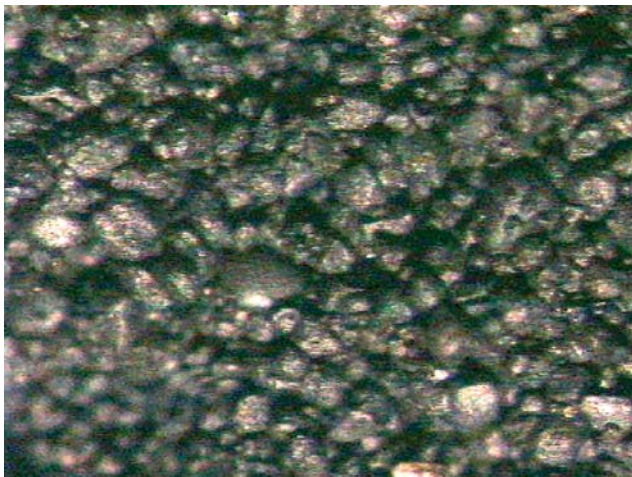


**Figure 1.** View of a mould wall

– the density of the material conglomerate. This “packing density” significantly influences the energy transport through the mould (Fig. 1). Therefore the average density of the mould should be considered at least.

The movement of the mould wall is mainly caused by the thermal expansion of the mould sand. But this expansion is only approx. 1 % within relevant temperature range, so that the amendment of packing density caused by this may be neglected on further calculation of heat flow.

### Heat capacity “apparent heat capacity” (c)

The heat capacity, that enters into the equations 2 in this case, is the heat capacity of a granular material conglomerate of mould basis material and binder system (Fig. 1). It is an “apparent heat capacity” applying at first only to the volume element with a certain voids fraction and a certain packing density, which underlies the measurement.

$$\rho c(T) \frac{\partial T}{\partial t} = \text{div}[\lambda(T) \text{grad} T] + \dot{W}(T, \vec{r}, t) \quad (2)$$

The influence of the inorganic binder to the heat capacity of this volume element may be neglected, as their portion is small and as there is not a big difference within heat capacity between mould basis material and binder.

The portion of organic binders within mould material systems is even smaller and their contribution to the heat capacity of the system, in which an oxygen deficiency inside of the pore volume avoids the complete combustion of the binders, results from required energy for disintegration and the energy set-free from combustion. This

energy contribution in the form of a heat source within the volume element might be negligible.

The enthalpy for the  $\alpha$ – $\beta$  allotrope change of the quartz is 10.5 kJ/kg and – compared with the heat capacity of the mould – is consequently negligible small too.

Inside wet sand the vaporization, the condensation and the migration of the condensation zone goes through the volume element at low temperatures at the beginning of the solidification. Therefore, at first a heat source (releasing condensation heat) goes through the volume element followed by a heat lowering (depriving heat of vaporization). These effects enter into the apparent heat capacity and there is no need to consider them specially.

This apparent specific heat or heat capacity respectively would be independent from  $T$  but would depend on the temperature at transition point metal / mould material and considers the heat absorbed from the mould completely.

### Thermal conductivity “apparent thermal conductivity” $\lambda$

In the same meaning as at heat capacity there results an “apparent thermal conductivity”. These “apparent thermal conductivities” would be different at the same sand and different casting alloys, such as aluminium, cast iron and steel. It results in a dependence of the apparent thermal conductivity from packing density and from the melting temperature of the alloy. The apparent thermal conductivity decreases on increasing voids fracture.

Within a lot of papers the specific thermal conductivity is defined as apparent specific thermal conductivity between room temperature and transition temperature at transition point metal / mould. But here the above-mentioned definition is used, as it considers the heat absorbed from the mould.

## **VARIABLE MATERIAL VALUES, WHICH DEFINE THE SOLIDIFICATION PROCESS**

### **Average carbon activity**

The average carbon activity of cast iron is mainly defined by the content of carbon graphite or carbide stabilizers as well as of the actual temperature. Within a certain range the degree of saturation and the carbon equivalent are rules for it.

### **Local carbon activity**

This means the carbon activity directly at the place of solidification. It is defined by the local composition which is defined by separation processes, liquation and undercooling.

### **Diffusion coefficient**

The diffusion coefficient of a cast iron is defined by the content of carbon, graphite and carbide stabilizers as well as by the actual temperature. There is no simple term like the degree of saturation to describe this value, but it defines the separation process of the two phases austenite and graphite during the eutectic solidification.

### **Diffusion path length**

The diffusion path length during the separation of the eutectic melt to austenite and graphite is arranged by the number of nuclei forming and able to growth. The diffusion path length only depends on the number of nuclei and not on their formation (theory of nuclei formation).

### **Growth of austenite and graphite**

The growth is defined by the thermodynamic values volume energy and interfacial tension.

## **INFLUENCE OF MATERIAL VALUES**

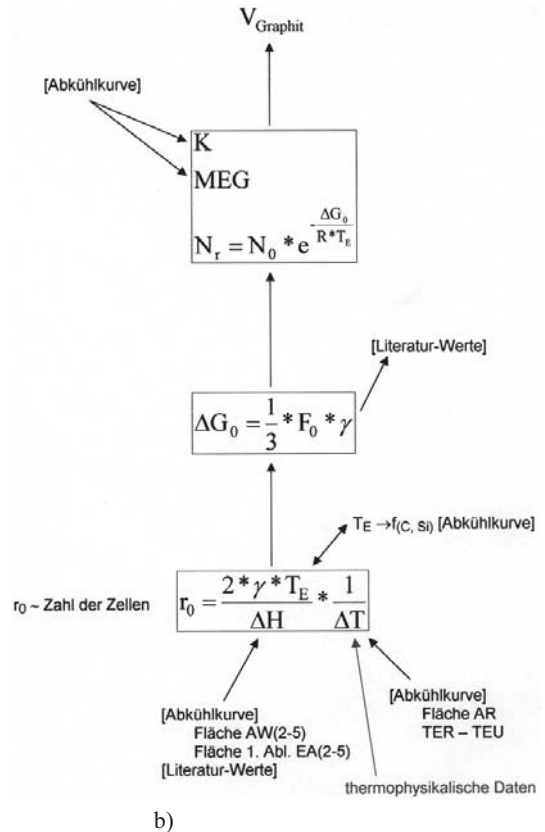
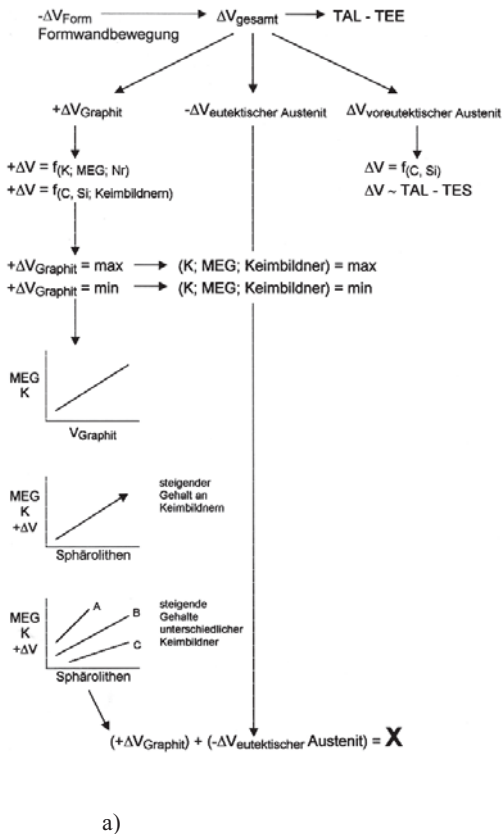
### **Material values and their definable structure**

If – in a first step – the shrinkage volume resulting from a mould wall movement are regarded as constant and not influenceable by the material, the total shrinkage volume results as additive sum of contraction volume of the hypoeutectic austenite the eutectic austenite and the volume increase of graphite at its precipitation.

The size of the hypoeutectic solidification contraction is mainly defined by the chemical composition, especially by the carbon and silicon content and values like the degree of saturation or the carbon equivalent respectively, in which further elements are considered. They are a degree how much the actual composition differs from the eutectic one (Fig. 2). Therefore the quantity of hypoeutectic solidification may be fixed by

the thermal analysis by means of the temperatures, which define the beginning and the end of the hypoeutectic solidification. A contraction volume can be derived from the weight or volume of the predictable

hypoeutectic solidification. This contraction volume can be equalized either by feeding or can be minimized by changing the chemical composition. The minimization of the contraction volume may be done by



$\Delta T$ :	Unterkühlung der Schmelze
$\Delta H$ :	Enthalpie
$T_E$ :	Temperatur der stabilen eutektischen Erstarrung
$\gamma$ :	Oberflächenspannung
$r_0$ :	Keimradius
$F_0$ :	Oberfläche des Keims
$\Delta G_0$ :	Freie Enthalpie des Keims
$N_r$ :	Zahl der kugelförmigen Cluster
MEG:	Menge des eutektischen Graphits
K:	Graphitisierungstendenz

Figure 2. Influence of the solidification manipulation for controlling the solidification contraction.



addition of carbon or silicon or by an amended inoculation modus.

The hypoeutectic solidification portion, defined by this way, fixes the quantity of the eutectic solidification as a complementary sum to the total volume or to the weight considered. The eutectic solidification consists of the eutectic austenite with a volume contraction and the graphite with a volume dilatation. Eutectic austenite and graphite are fixed in their mutual relationship according to the multiple component system. By this the contraction sum of the eutectic austenite becomes a calculable value (Fig. 2a).

The only value, which is now decisive for the decrease of the eutectic shrinkage volume, is the quantity of the precipitated graphite with the corresponding volume increase. At first you have to avoid the possibility of the meta-stable solidification of eutectic that would be combined with a non-compensation of the eutectic austenite contraction. As a rule this is done by adjustment of the carbon and silicon contents to the wall thickness and by adding inoculants that initiate the precipitation of graphite. The quantity of eutectic graphite and consequently the size of volume increase is a function of carbon and silicon contents. The number of spheroids is a question of the number of nuclei, as the same graphite volume may divide to one great spheroid or to any number of small ones. The efficient number of nuclei results of the content of inoculants and the combination of efficient components within inoculants (Fig. 2a).

Without entering nucleation theories it is possible – by means of known data from literature of surface tension and enthalpy of

fusion – to make calculations, which may lead by support of the thermal analyse to statements about number of nuclei and the approximate graphite volume (Fig. 2b).

### **Influence of moulding material values**

The real feeding demand of a casting consists of:

- volume deficit of the hypoeutectic contraction,
- volume deficit of the eutectic contraction,
- volume increase of the eutectic graphite precipitation and
- “apparent shrinkage”.

The “apparent shrinkage” is a value that is only found within a few reflections for feeding calculations so far. To carry out this paper it was consequently necessary to define the possible influence factors of the “apparent shrinkage” exactly.

The “apparent shrinkage” is a magnification or enlargement of the mould cavity due to the casting process, the solidification behaviour of the cast iron and the attributes of the mould material (mould wall movement). These influences may increase the feeding demand of the casting.

The “apparent shrinkage” consists of two main influence factors:

- the load defining the pressure onto the mould wall produced by the casting process and the solidification behaviour of the cast iron (graphite precipitation),
- the enlargement of the mould cavity or the stability of the mould that withstands the pressure (mould wall movement).

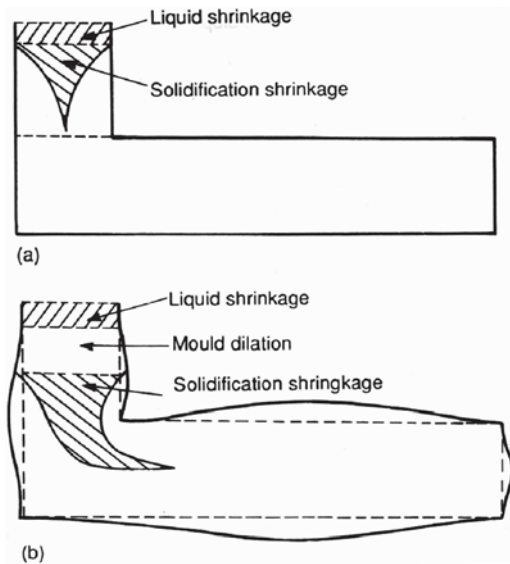


**Figure 3.** Interaction between solidification and shrinkage in a mould:

- a) the apparent shrinkage does not appear,  
 b) the apparent shrinkage appears.

Figure 3 shows shrinkage cavities appears when the feeder does not have enough liquid iron for compensation of apparent shrinkage, a) no mould wall movement, shrink-free casting, exactly according to pattern, sufficient

feeding volume b) great mould wall movement, casting larger than pattern, shrinkage within casting, insufficient feeding volume.

The graphite precipitation or the solidification behaviour of cast iron with spherical graphite is not the only parameter that defines the pressure onto the mould wall. Other loads developing on casting and solidification process are big figures too.

These loads result of:

- the ferrostatic pressure,
- the casting heat,
- the composition of alloy.

The second main influence factor defining the apparent shrinkage is the mould movement or the mould attributes respectively. The dependences of the mould wall movement result of:

- the type of mould material,
- the composition of mould material,
- the compaction,
- the geometry of the mould,
- the attributes of the mould box.

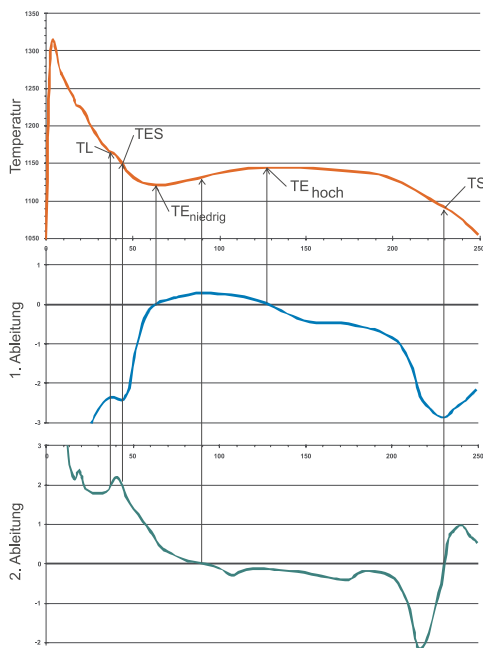


# **PART 2: SOLIDIFICATION STRUCTURE OF CAST IRON** **AND EFFICIENCY OF FEEDERS**

## **THERMAL ANALYSIS**

From the 1<sup>st</sup> derivative of the cooling curve results the gradient of the cooling rate over the complete solidification process. The point where the cooling rate (the first derivate) shows the first maximum and starts to decrease again corresponds to the liquidus temperature TL. The following first minimum is the temperature for the beginning eutectic solidification, the eutectic start

temperature TES. The TES following point of intersection of the 1<sup>st</sup> derivative and the zero line marks  $TE_{low}$ . At this point the dissipated heat and the released latent heat are in balance. From this point the released latent heat of graphite precipitation prevail and this leads to temperature increase. After a now following maximum of the first derivative the cooling rate decreases again and shows a zero value corresponding to  $TE_{high}$ . After this the ongoing eutectic solidi-



0	TL	1	LIQUID TEMPERATURE, IT IS THE TEMPERATURE WHERE THE FIRST SOLID PARTICLES APPEAR, NORMALLY AUSTENITE AS A CONSEQUENCE OF COOLING IN THE CAST IRON
2	TES	3	START TEMPERATURE OF BEGINNING EUTECTIC SOLIDIFICATION
4	$TE_{LOW}$	5	THE MINIMUM EUTECTIC TEMPERATURE AFTER THAT TEMPERATURE INCREASES AS A RESULT OF RELEASED LATENT HEAT
6	$TE_{HIGH}$	7	THE MAXIMUM EUTECTIC TEMPERATURE AS A RESULT OF THE RELEASED LATENT HEAT
8	TS	9	SOLIDUS TEMPERATURE, THE TEMPERATURE WHEN THE SOLIDIFICATION PROCESS IS FINISHED
10	$T_{METAST}$	11	TEMPERATURE OF METASTABLE EUTECTIC SOLIDIFICATION
12	R	13	RECALESCENCE - DIFFERENCE OF TEMPERATURES $TE_{LOW}$ AND $TE_{HIGH}$

**Figure 4.** Significant points within cooling curve of cast iron

fication ends at point TS, indicated by a minimum at the first derivative.

The first derivative is also in a position to define the periods of solidification. The period of hypoeutectic austenite solidification results up to the first minimum, which is marked by the length growth of the dendrites. The first minimum represents the moment when the eutectic solidification begins and between minimum and crossing zero-line the austenite dendrites are growing thicker instead of growing in length. This process is coupled with a eutectic solidification at the same time. This pure eutectic solidification is defined by this zero crossing and the zero crossing of the second derivative at the end of solidification.

The possibility of metastable eutectic solidification is marked by the metastable eutectic temperature, which can be calculated with different factors. If  $TE_{low}$  falls below this specific temperature, which is strongly

influenced by Si and elements stabilizing carbide, this may lead to a metastable solidification with a corresponding higher volume deficit. Due to carbide decomposition during further solidification process this chill must not be positively recognizable at room temperature. Therefore  $T_{metast}$  should be lower than  $TE_{low}$ .

Likewise there can arise a shift to metastable solidification at the end of the solidification process by an enrichment of alloying elements within remaining melt. The final temperature of the eutectic solidification should be above those of the metastable eutectic temperature.

The height of (TL) liquidus temperature as well as the period of time until temperature  $TE_{low}$  will be reached are a degree for the quantity of hypoeutectic austenite solidification and – proportional to this – for a feeding demand. This feeding demand can only be equalized by a feeder. This volume

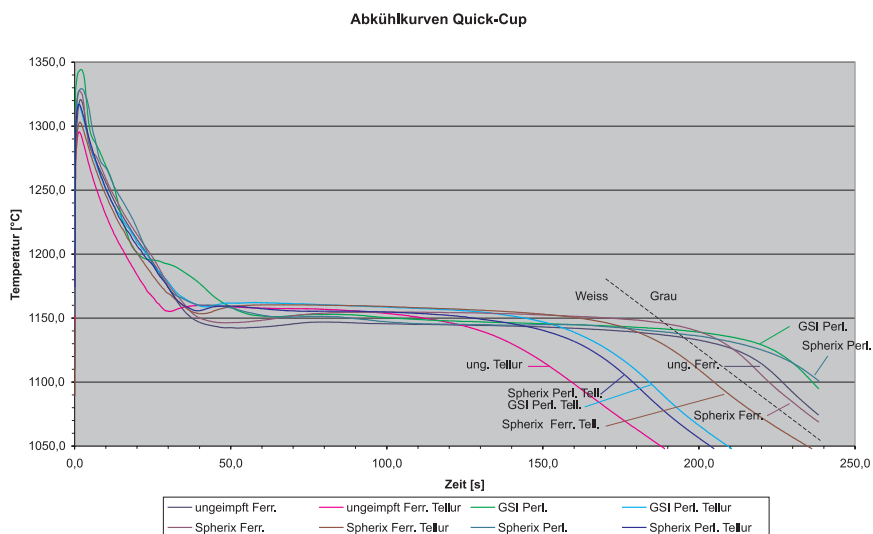


Figure 5. Some real cooling curves.

deficit of solidification cannot be reduced by the following graphite precipitation. Within this phase – after the austenite dendrites have built a spongy network structure and thereby have defined the future surface resp. wall structure – there is at first the diameter growth of the dendrites and the beginning precipitation of graphite between the dendrites with a corresponding volume increase. In this connection exists the possibility resp. the danger of an enlargement (growth) of casting areas with an increasing inner volume deficit. Therefore TL should be as low as possible and the period between TL and  $TE_{low}$  should be as short as possible.

The recalescence R is the difference between  $TE_{low}$  and  $TE_{high}$ . It represents the released latent heat of the eutectic solidification. The recalescence should be as low as possible,

and  $TE_{low}$  as well as  $TE_{high}$  should be clearly above  $T_{metast}$ . Steady and good graphite precipitation can be expected then that would correspond to the conditions for self-feeding or riserless pouring technique.

Real cooling curves show characteristic differences with regard to their nucleation condition and the cooling conditions (Fig. 5).

From reflections on solidification and solidification morphology the different significant temperatures and time periods of the cooling curves have to point out, which structure as well as which volume deficit have to be expected (Fig. 6). With today's computer facilities it is possible to define the single periods of time and temperature also by a 1<sup>st</sup> and 2<sup>nd</sup> derivative of curve already during recording the solidification curve and to

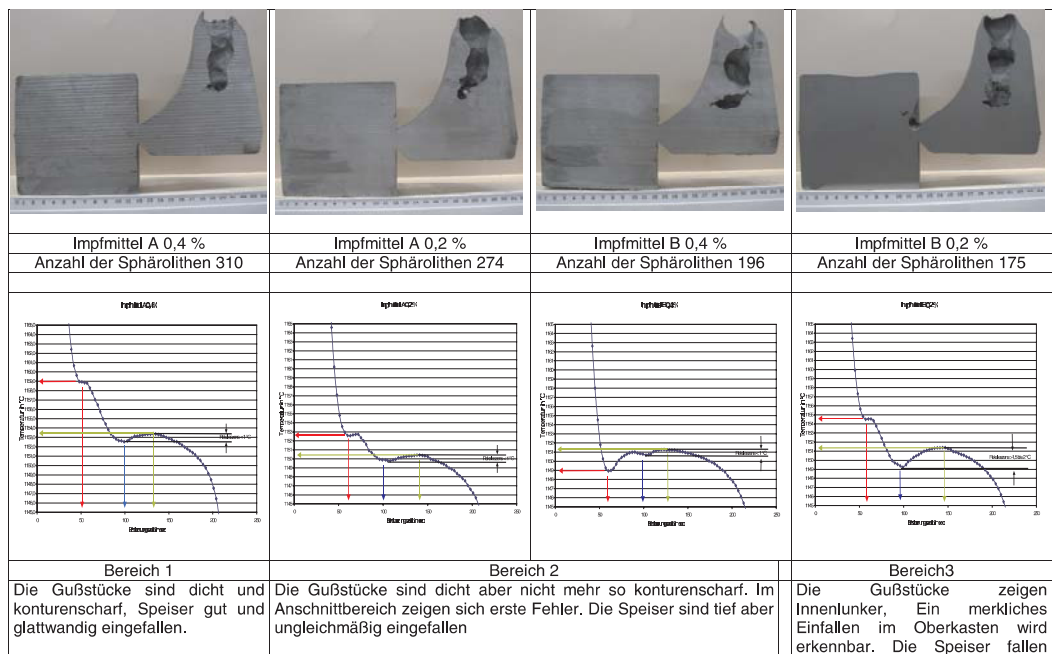
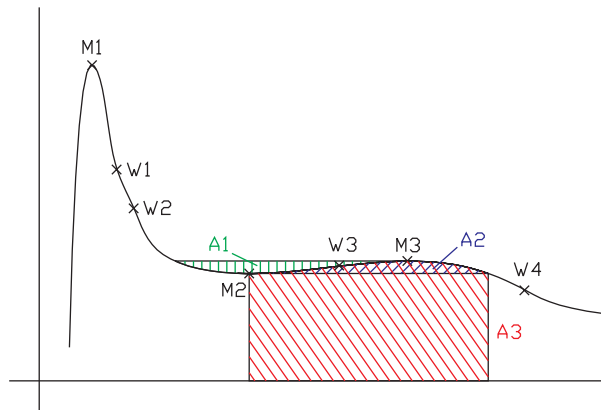


Figure 6. Real cooling curves in comparison to casting results.



**Figure 7.** Scheme of points and areas of evaluation in comparison with structure evaluation

transfer them to a analysis of variance, from which a correction measure has to be derived.

According to Figure 7 evaluation programmes have been made for the melts in question, and it was tried to state dependences.

## TIME FRAME OF FEEDER EFFICIENCY

### Feeding is a transport phenomenon

Feeding is founded on transport processes of flowable material from the feeder into the contraction areas of the casting to compensate there the arising volume deficit. This means that in the casting, too, corresponding transport processes have to take place. These necessary transport processes are restricted by the solidification morphology of the alloys. At a cast iron with spheroidal graphite several crystallization processes with different morphologies take place one after the other.

The primary solidification of cast iron is always exogenous spongy up to mushy. Already at an early stage a dendrite network

passes through the casting wall and builds a spongy plating, in which the remaining eutectic melt solidifies.

Spheroidal eutectic solidify endogenous mushy. The graphite spheroids will be enclosed by growing austenite and will be isolated from remaining melt. By diffusing carbon through the austenite to the graphite spheroid this spheroids can grow and can affect a strong pressure to their surroundings. This effect will be stronger and for a longer period of time the longer the solidification time is or the longer the wall / casting remains in liquid condition.

Feeding types differ according to:

- mass feeding,
- interdendritic feeding,
- feeding by sucking solidified shells inwards (surface sinks),
- self-feeding – compensation of the metallic solidification contraction by the volume increase of precipitating graphite.

**Mass feeding** is the movement of a mixture of crystals and melt from the feeder into the casting due to gravity. This process come to an end as soon as the crystals hinder each other in their movement, hook or jam, this is the so-called “pour point”. There are a direct coherence between feeding capacity and solidification morphology. The mass feeding is mainly responsible for the formation of macro-shrinkage within feeder.

**Interdendritic feeding** is the movement of melt through a crystal network. With their quantity portion at feeding it is defined by the ramification degree of the crystals and the resulting flow channels. Within interdendritic area conditions are to assume like within a filter, at which the size of flow channels at a point of time X is defined by volume relation between crystal network and melt. Portion of interdendritic feeding at total volume of a macro-shrinkage has to be estimated as small.

**Feeding by sucking solidified shells inwards (surface sinks)**, as movement of two opposite surfaces to each other, can only avoid the formation of an inner deficit and for the present it has no perceptible influence to the formation of macro-shrinkage within feeder. Surface sinks often are not macroscopic perceptible offhand.

**Self-feeding** as a compensation of metallic volume contraction by volume increase of self-precipitating graphite within a melt has to be regarded in a direct coherence between the quantity of self-precipitating graphite and the quantity of hypoeutectic and eutectic austenite, so that the contraction of austenite can partially or completely be compensated by the volume increase of graphite, or may be even exceeded. The latter is known as a swelling or growing of castings combined with a volume increase of the castings.

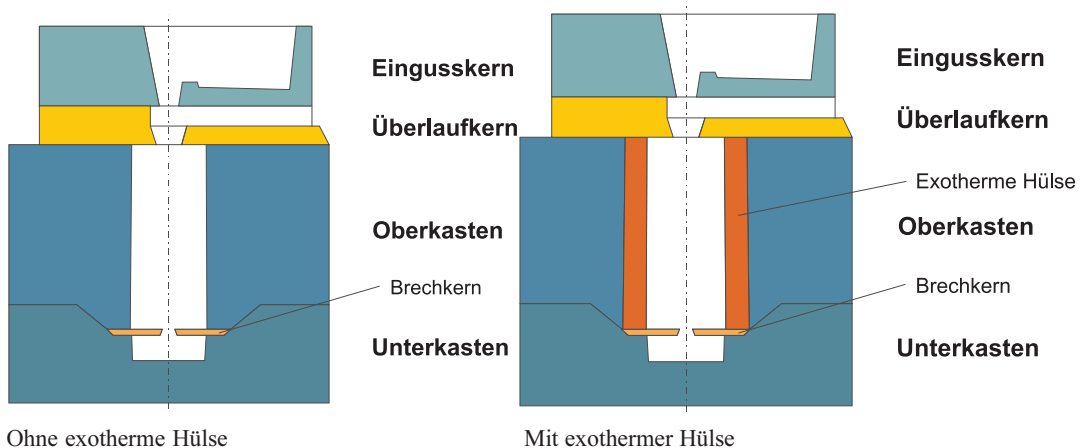


**Figure 8.** The assembly – pour point investigation.

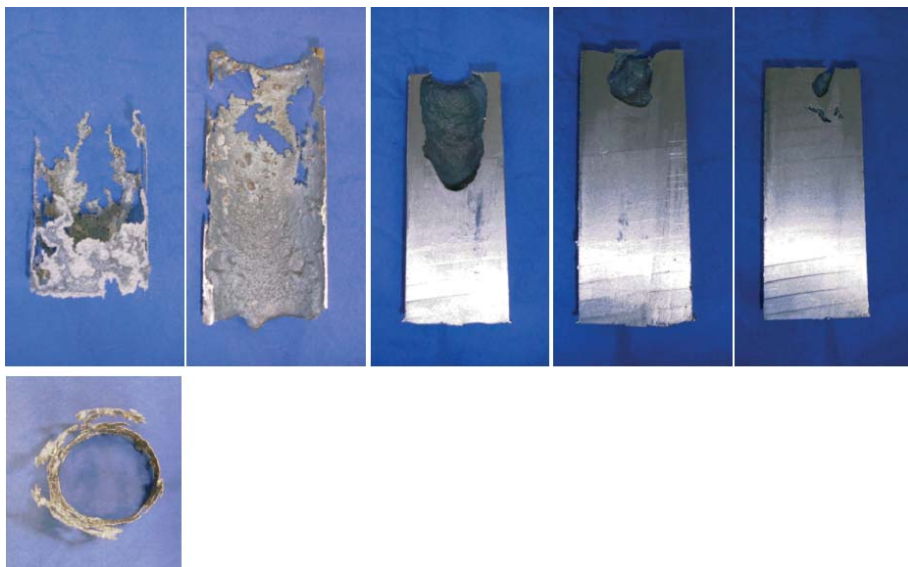


**Figure 9.** Several Points of time during solidification.

### Pour point

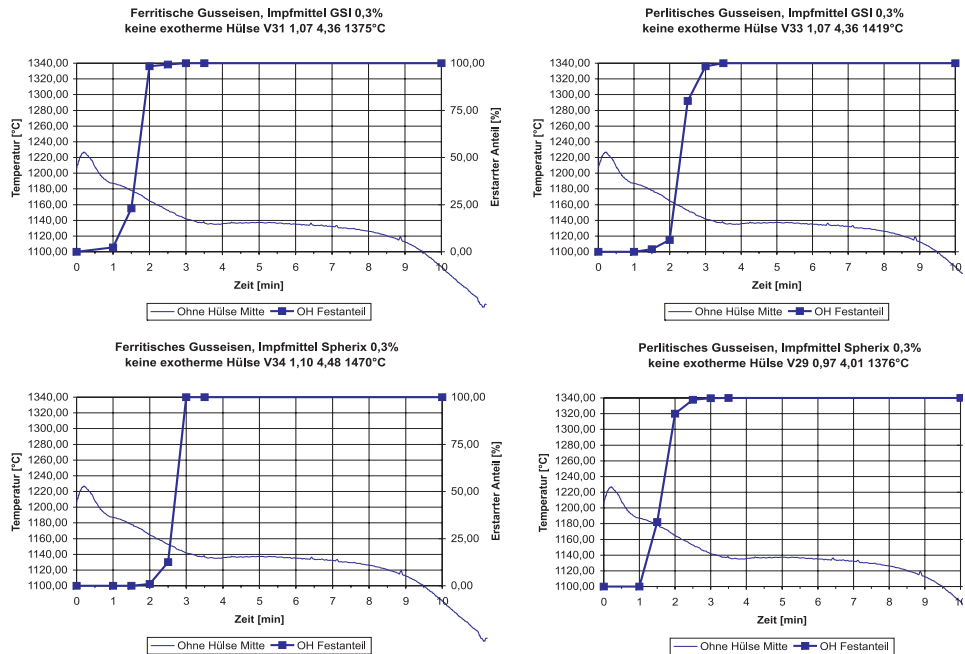
Figure 8 schematically shows the experimental set-up. This set-up was oriented on an experimental arrangement, which already has been used in a similar way. The test-piece, in principle representing the feeder, was arranged within a cope box, a cam with separating core were arranged within a drag box. Sprue-core and flow-off core are set on the cope box. The sprue-core, flow-off-core and separating-core were made of  $\text{CO}_2$  sand or furan resin sand. There were used common production resins without additives. The sprue-core had the function to enable a uniform filling of the test-piece and to position the flow-off-core above the test-piece. The flow-off-core took care for a constant filling level of the test-piece. Surplus material from the sprue-core flew-off over the rear side of cope box after effected filling of the test-piece. This led to

uniform test conditions (no feeding effects). The cam and the test-piece heat the separating core (principle of a breaker core below a feeder) and thereby decrease the cooling speed at the bottom side of the test-piece. In this area the test-piece solidifies more slowly. Now it is guaranteed that material which is still being moveable inside the feeder will flow-out by taking off the feeder. Figure 9 shows several points of time during solidification.

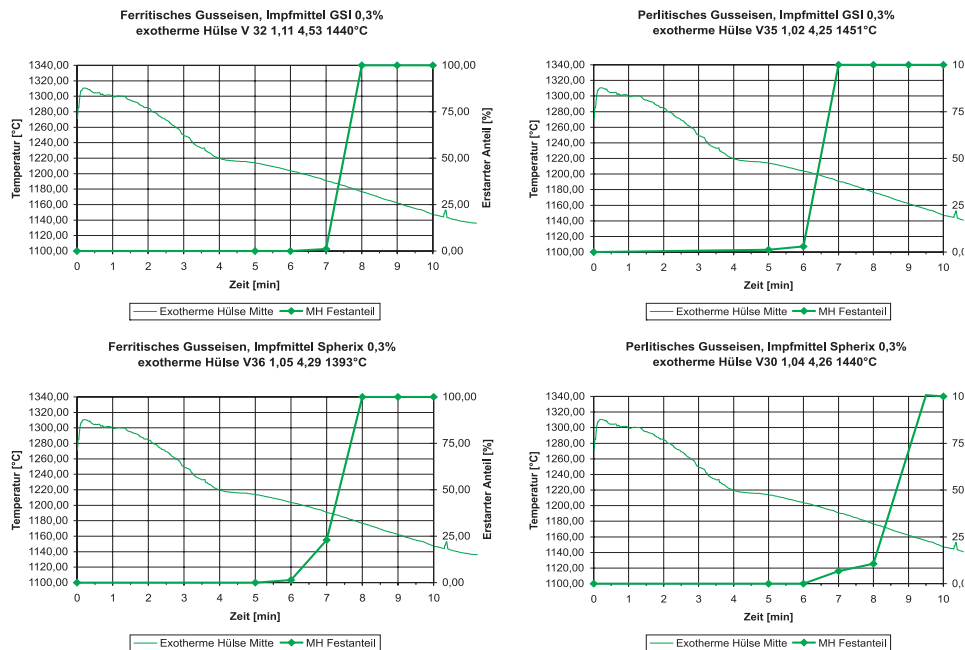
### Conclusions of the results of the pour point test (Fig. 10)

Under same conditions pearlitic and ferritic iron become immovable approx. at the same time. For both cast iron qualities the possibility of a mass feeding is finished already before the beginning of eutectic solidification. The volume deficit occurring during further solidification of metallic





a) without exothermic sleeve



b) with exothermic sleeve

**Figure 10.** Quantity of the solidified portion a) without and b) with using an exothermic sleeve, registered in the solidification curve.

matrix may then only be compensated by

- interdendritic feeding,
- feeding by surface sinks,
- self-feeding,

i.e. by volume increase of the eutectic self-precipitating graphite. This should have the main influence with regard to the density of a casting, because the feeding possibility within interdendritic area for longer distances is not possible without corresponding pressure differences (analogy to filter), and a sinking of the walls should become impossible, too, with a dendrite self-supporting network existing all over the complete cross-section of the wall.

So a feeder at cast iron with spheroidal graphite can only compensate the liquid contraction from casting temperature up to the beginning of solidification as well as a part of the volume contraction of the hypoeutectic austenite solidification. After starting eutectic solidification there is no moveable metal in the feeder. The main rest of volume contraction of the solidifying metallic matrix has to be compensated by the volume increase of the self-precipitating

graphite. This quantity may – among others – be controlled by composition, graphitization potential and cooling speed.

With regard to the solidification simulation it results that the early immovability of the mass within feeder has to be considered, as it is only possible to give an accurate prediction when it is known how long a feeder can supply movable material at different iron qualities. Resulting change of shifting thermal centres due to gravity ends at this time. The principle of directional solidification and its corresponding simulative translation cannot be maintained for cast iron after this point of time, this means approx. 20 – 30 % of the total solidification time at both ferritic and pearlitic cast iron. Thermal centre still existing or still arising at this point of time have to be criticized with the consideration of volume increase of graphite at a controllable eutectic graphitization potential. This must be different to the eutectoid graphitization potential with the consequence of ferritic and pearlitic cast iron.

### PART 3: INFLUENCE OF COOLING CONDITIONS AS WELL AS OF INOCULATION TO THE SOLIDIFICATION STRUCTURE

#### CASTING METHOD

The hot-wire method as a measuring method to analyse thermo-physical data of refractory material is only conditionally suitable to analyse thermo-physical data of the moulding material, as the values analysed by this method do not reflect the conditions within the mould during casting. The long heating times, necessary for this method due to the necessity of a temperature balance, lead to modifications within mould material. At each measurement at more than 100 °C or even at nearly 100 °C the moulding material will be completely dried. At higher temperatures the lustrous carbon former pyrolyse, and the bentonite, too, changes due to loss of chemically combined water. These processes, which may have effects to the heat transfer within the mould, do not take place within the mould in this way, at least not at a greater distance to the casting or within the time between pouring and formation of a rigid outer shell.

Furthermore, it is hardly possible to effect measurements under operation conditions according to the hot-wire method. Due to the fact that the thermo-physical data also depend on the packing density of the mould material and therefore depend on its compaction, the mould – as a consequence – has to be produced by a moulding machine under operation conditions. Afterwards, the hot wire would have to be built into the mould, and the complete mould box would have to be put into the furnace for analyse of the temperature dependence.

An alternative to analyse thermo-physical data – especially under operation conditions – is the casting method. This method is useful for analysis of thermal diffusivity.

$$a = \frac{\chi}{\rho c_p} \quad (3)$$

This value describes the speed, by which a temperature modification spreads within mould material.

The analysis of the thermal diffusivity is made by the casting method by measuring the spreading of a temperature front within mould material. Although in general an analytic solution of the heat conductivity equation is not possible a solution can be found for simple special cases, especially for one- or two-dimensional problems. These cases can be approached to a test by using a geometrical simple body – for example a cube, a plate or a cylinder. Such a mould is poured and during solidification and cooling process the temperature is measured at different distances to the casting wall within mould material. Design and size of the test body are chosen in such a way to achieve a temperature distribution within mould material, which will be easily to describe. This will only take place if the distance between measuring position and casting wall will be small compared with the expansion of the casting wall releasing heat. If a one-dimensional temperature distribution is achieved (i.e. the temperature only depends on the distance from measuring position to

the casting wall) it is possible – by laying down the heat balance – to calculate thermal diffusivity according to

$$a = \frac{(T_{2b} - T_{2a}) \cdot \left( \left( \frac{r_2 + r_3}{2} \right)^2 - \left( \frac{r_1 + r_2}{2} \right)^2 \right)}{2 \cdot \Delta t \cdot \left[ \frac{T_1 - T_2}{\ln \left( \frac{r_2}{r_1} \right)} - \frac{T_2 - T_3}{\ln \left( \frac{r_3}{r_2} \right)} \right]} \quad (4)$$

At which  $r_1$ ,  $r_2$ ,  $r_3$  are radii of the three measuring positions,  $\Delta t$  is the relevant period of time,  $T_1$ ,  $T_2$ ,  $T_3$  are the average temperatures of the three measuring points within this section, and  $T_{2a}$  and  $T_{2b}$  are the temperatures of the middle measuring point at the beginning and at the end of this period of time.

There are possible measuring points within mould material in front of the middle of a plate or a cube surface; easier measuring conditions are given at a cylindrical test body. By using a rotation symmetry several measuring points may be arranged around the test body (Fig. 11), and by taking the average of measured curves it is possible to reduce the effects of insecurities of measuring positions and other faults of measuring. The figured test arrangement represents the optimum.

Due to mould technical reasons the test body cannot be a perfect cylinder, as a certain inclination of mould is necessary to remove the pattern from the produced mould. For measuring the temperature distribution within mould material there are used thermo couples without protection covering, which are set into boreholes of less than 2 mm

diameter within mould material. Due to the small mass of these thermo couples they can quickly follow up modifications of mould material temperature.

The thermo couples are set into blind holes, which are cut into the mould material from the mould joint by using a strickle. As the thermo couples are led from the measuring point (tip of the thermo element) up to the mould joint at a parallel way to the casting

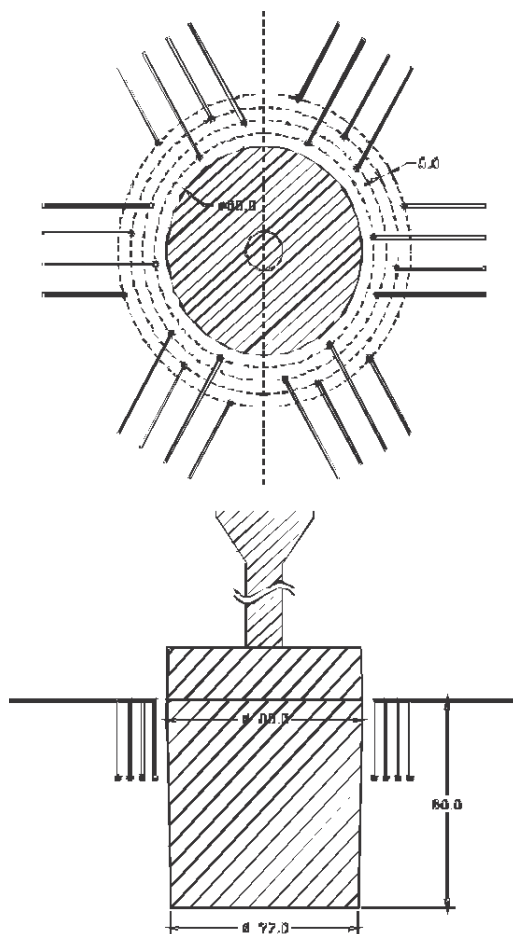


**Figure 11.** Arrangement of measuring positions at a rotationally symmetrical experimental set-up.

wall and by that alongside the isothermal line, a falsification of the measuring values by the heat conduction of the thermoelectric wire can be avoided. The lead-in wire of the thermo couples are led to the outside alongside the mould joint and are connected with a multichannel data logger (Fig. 12). Due to the grain structure of the mould material as well as due to its rather low strength the positioning of the thermo couples cannot be done as accurate as desired. This is the reason

for using 6 trial equipments (each 4 thermo couples) equally placed around the test pattern (it was measured at a distance of 5, 10, 15 and 20 mm from mould wall).

The average of these 6 temperature curves achieved by this method was taken, whereby the highest as well as the lowest measuring value have been ignored. Within mould material result the following temperature curves (Fig. 13).

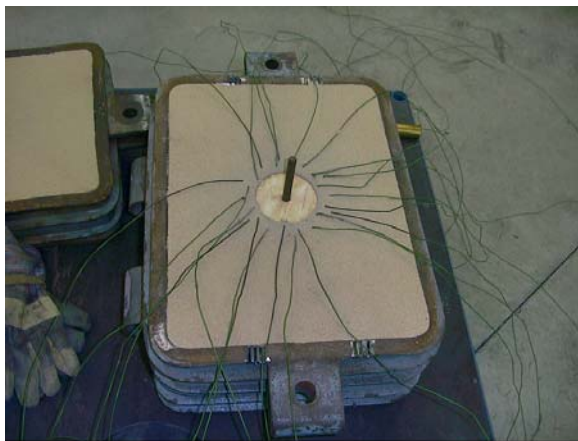


**Figure 12.** Design of experiments.

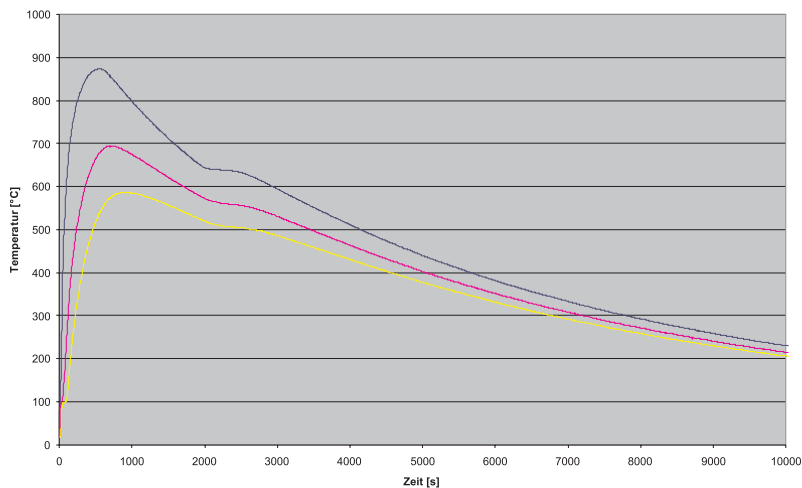


**Figure 13.** Average temperature curves within mould material.

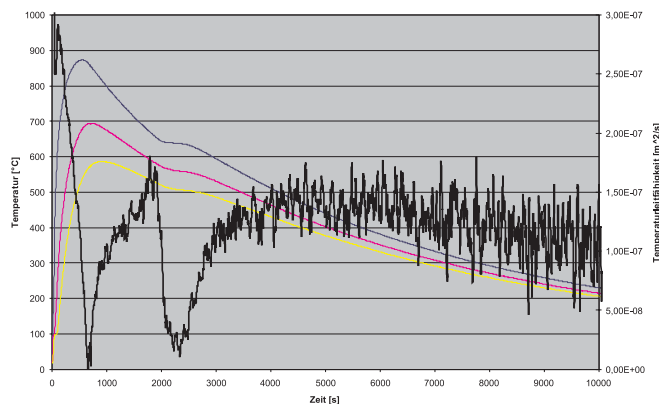


**Figure 14.** Calculated temperature diffusivity during test phase.

From this temperature curves the thermal diffusivity during test phase can be continuously calculated. Only the area of cooling phase has been evaluated, because after pouring the liquid metal into the mould there are further processes, which influence the measurement and the evaluation. So an arrest point of 100 °C can clearly be recognized at the beginning of all temperature curves, after that the temperature rises again and shows a course, which corresponds to a heat transfer by means of thermal conductivity. The arrest point is caused by the displacement of water, which was used for bonding purposes. This

is the reason for not using this area within the calculation of thermal diffusivity. A second area at which the measurement cannot be evaluated is within figure 14 approx. 2000 up to 2400 seconds. During this time period a latent heat that compensates the cooling for a certain period of time is set free within the casting. During the further course of the measurement temperature differences become smaller and smaller, so that the relative measuring error continuously rises, until at least, at low temperatures, no more evaluation will be possible.

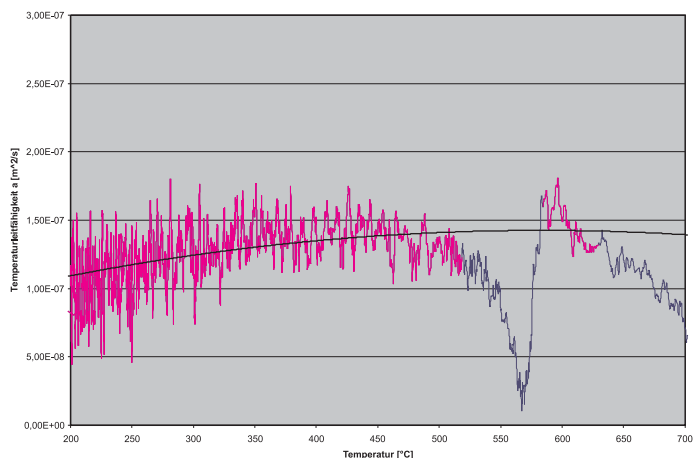


**Figure 15.** Calculated temperature dependence of temperature diffusivity



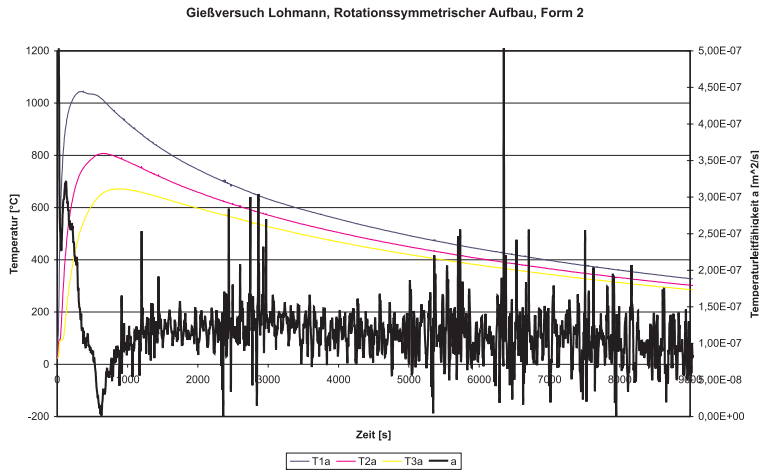


**Figure 16.** Temperature curves of steel

If the calculated temperature diffusivity is figured above the average temperature taken within mould material (in the area of measurement points) it results to Figure 14.

The gap, within calculated temperature diffusivity curve, corresponds to the above explained arrest point due to set-free latent heat. But it is easily possible to define a compensation curve that bridges this area (Fig. 15).

By using a single test it is possible to define the thermal diffusivity of mould material for a large temperature range (here: 200 up to 700 °C). Nevertheless the evaluation of the used mould material – consisting of silica sand with 8 % bentonite and adjusted to a compactability of 45 % - shows a rather small temperature dependence of thermal diffusivity. Similar results have been achieved on further tests, among other things with production mould materials of participating foundries.

As expected, the steel tests do not show the described arrest point of temperature curves. The reason is the different solidification behaviour of steel.

At each participating foundry two measurements had been done (Fig. 16).

It is conspicuous that at each second measurement were always analysed higher thermal diffusivity in the three foundries for all test runs. This may eventually refer to the fact, that the moulds were produced directly one after the other, i.e. with an interval of several minutes, according to machine cycle time. But the positioning of the thermo couples and the connection to the data logging device took approx. 30 minutes per mould, so that – although the second mould had been immediately covered – a drying resp. modification of mould material by souring effect could not be excluded in the course of time.

## INFLUENCE OF DIFFERENT COOLING CONDITIONS TO SOLIDIFICATION

The different thermal diffusivities of the mould material, i.e. its different cooling effect and by that a different cooling rate

within casted metal – even at same conditions – may cause different structures and by that different shrinkage sensitivities. The effects, which may have even small differences within cooling rate, are shown in Figure 17. In this diagram the relationship is shown between the volume contraction and the degree of saturation. It should be noted that a volume expansion can only take place in a small range of the degree of saturation, defined by Si-contents, and this only for the stable eutectic solidification, i.e. for low cooling rate. At higher cooling rates the curves rise up, so that no more volume expansion can take place within short time, even not at an optimum degree of saturation of 1. Therefore a limitation of cooling rate is necessary to secure a self-feeding.

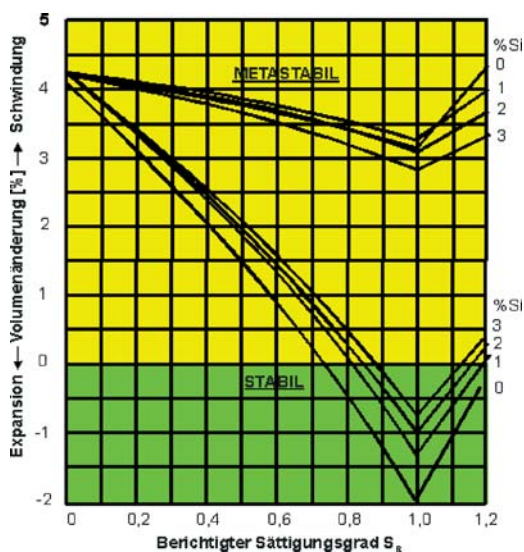


Figure 17. Theoretic volume modification of cast iron

It is apparent that the concept of the degree of saturation is not only sufficient for description of volume modification and by that for the formation of shrinkage, i.e. the figure of carbon with regard to the graphite

precipitation cannot be replaced for example by silicon, as it has been done at corresponding calculations of CE and Sc values.

But it also shows that at same chemical composition in a first step there cannot be differences between a pearlitic and a ferritic cast iron with regard to structure, volume modification and thereby shrinkage behaviour. Ferritic and pearlitic amount will not be fixed before eutectoid transformation in solid condition.

Between the group of curves of stable and metastable solidification there is the area in which the structure will be defined by the cooling rates thereby the shrinkage behaviour, and that will be the result of thermal diffusivity of mould material and the set-free heat quantity of the test piece.

But this process is – at same carbon activity within the melts - highly defined by diffusion, diffusion length and the growth rate, because in opposite to the ledeburite formation the graphite precipitation is a kinetic problem. The lower group of curves shows the optimum of an inoculated stable solidification with the effect of self-feeding.

A continuous transition is possible between both groups of curves, which may be expressed at the castings in form of hard spots or carbides within structure. Each part of carbide or ledeburite within the structure increases the feeding demand in opposite to the optimum. Due to the following transformation and precipitation processes in solid it might be these processes during cooling will not be recognized within metallographic evaluations at room temperature.

The adjustment of different cooling rates by variation of thermal diffusivity of mould material - for example by different compactibilities or mould material compositions - is only hardly to realize in practice. A pattern plate with test castings had been made to control the dependences. By one pouring there could be casted plates with a thickness of 10, 20, 30 and 40 mm, a cube with module 1.6 as well as a transverse link for cars (Fig. 18).



**Figure 18.** Cluster with test castings



**Figure 19.** Stepped wedge

The different plate thicknesses led to different moduli and by that to different reproducible cooling rates. The transverse links for cars were sawed, and the shrinkage was compared with known fault protocols of the foundry, but the results will not be shown at this place. Parallel to this stepped wedges were casted and compared (Fig. 19).

During the tests there were casted:

- ferritic and pearlitic adjusted cast iron,
- with each 2 different inoculants.

By these it was varied:

- carbon activity,
- diffusion coefficient,
- diffusion length,
- austenite resp. graphite growth.

Whereby further parameter were hold on a constant level for example degree of saturation, mould material composition etc..

Three test pieces were taken from each cube or plate, each one of the top (near mould joint), from the bottom and from the middle.

These test pieces were polished and they were evaluated by using a image analysis program with regard to the parameter:

- number of spheroids (recognized spheroids per  $\text{mm}^2$ ) and
- graphite quantity (percentage at surface).

As an example, Figures 20 and 21 show the influence of different wall thicknesses (and by that different cooling rates) to the formation of spheroids.

There are remarkable differences within the single structures. By increasing wall thickness and by that by decreasing cooling

speed the number of spheroids decreases, but their diameter increases. Especially inoculant B seems to have its optimum effect at a wall thickness of 30 mm.

CASTING IN PLATE DESIGN

At left side the Figure 22 shows pearlitic cast iron and in comparison ferritic cast iron at right side. The upper diagram shows the

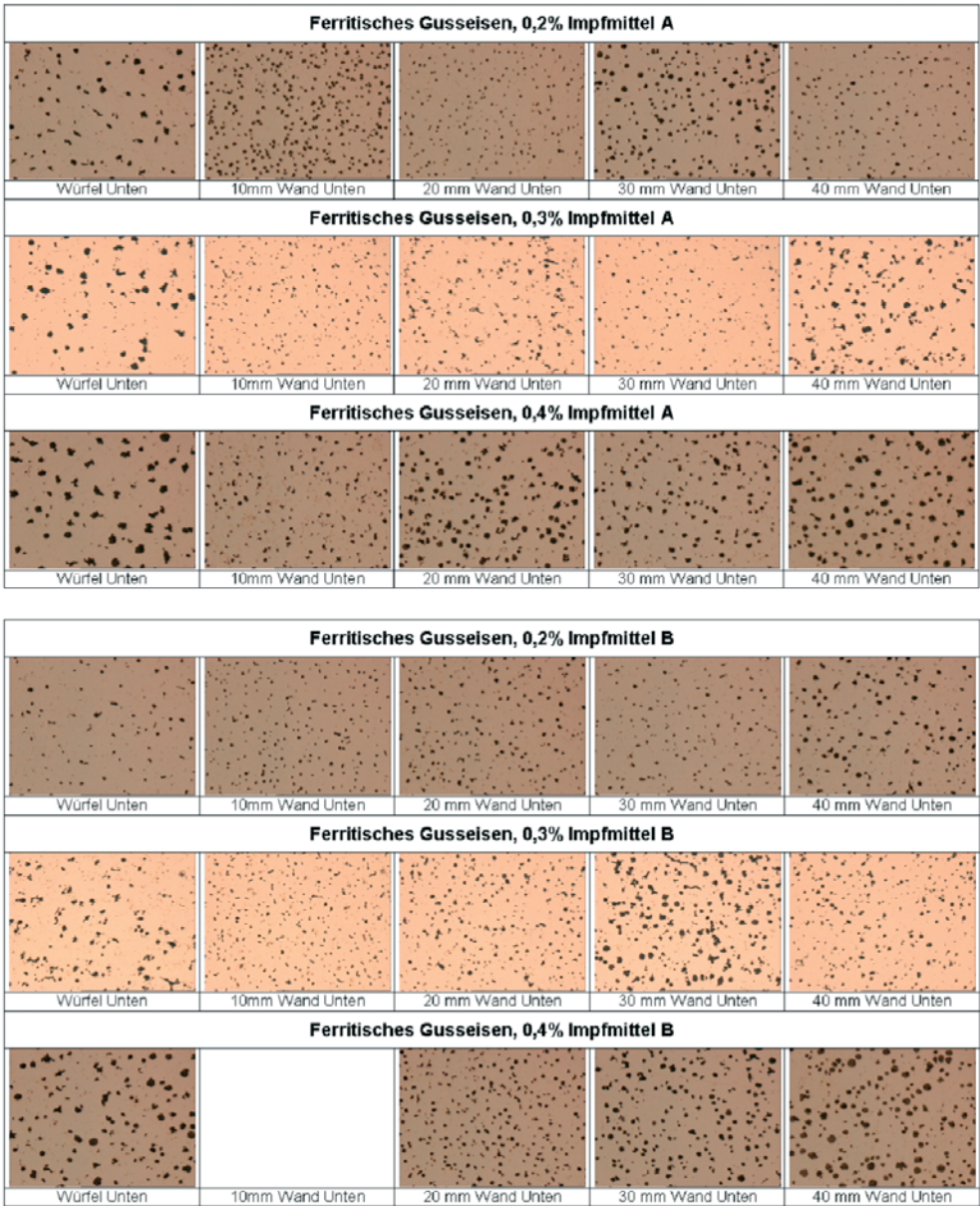


Figure 20. Ferritic ductile, inoculated with inoculants A and B



number of spheroids, the lower diagram shows the surface component of spheroids in percentage. Within each diagram inoculants A and B are shown in comparison.

At pearlitic cast iron it is clearly to see, that at same type and concentration of inoculant a higher cooling speed (at lower wall thickness) leads to an increase of the number of spheroids. The evaluation of surface component does not show a uniform tendency.

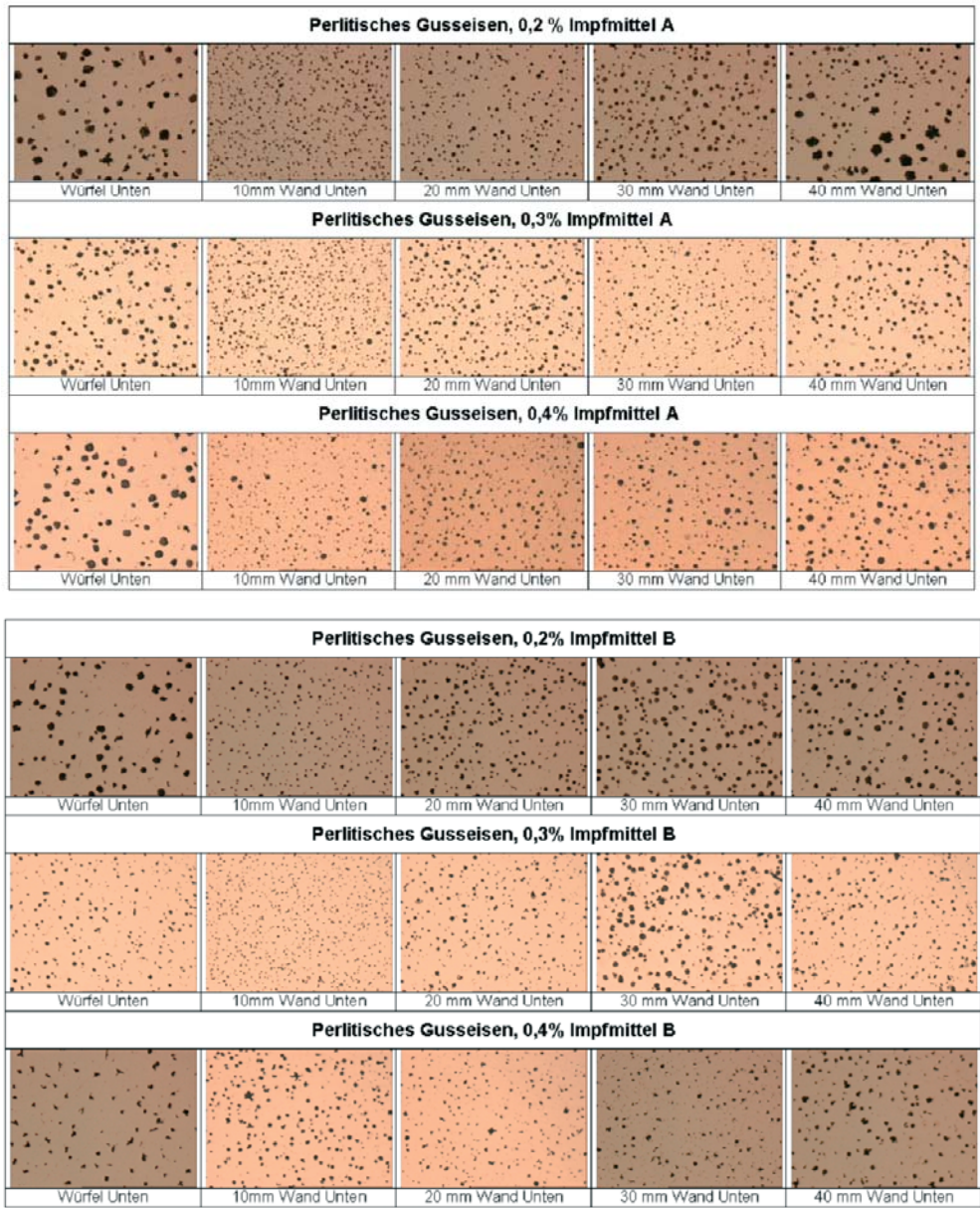


Figure 21. Pearlitic ductile iron, inoculated with inoculants A and B

At ferritic cast iron the dependence of the number of spheroids from cooling rate is remarkably lower. Here, too, the surface component does not show a uniform relationship between wall thickness or concentration of inoculant.

At both types of iron an inoculant concentration of 0.3 % results to an optimum number of spheroids. At higher inoculant concentration the number of spheroids decreases again.

## STEPPED WEDGE

Giving same inoculant at same concentrations the quicker type of cooling shows a remarkable higher number of spheroids (Fig. 23). Beginning at a wall thickness of 30 mm this tendencies efface a little and are not longer clearly. No basic difference is to recognize between inoculant

A and B. Inoculant B tends a little to a lower number of spheroids.

On increasing addition of inoculant the number of spheroids decreases at pearlitic cast iron. At ferritic cast iron inoculant A shows the same tendencies like pearlitic cast iron, but at a remarkable lower number of spheroids. At ferritic cast iron and at different inoculant additions inoculant B shows contrary behaviour to the use with pearlitic cast iron. The number of spheroids increases with increasing inoculant quantity.

On increasing inoculant addition the surface component of spheroids decreases at both inoculants. For inoculant A there is no difference to recognize for all wall thicknesses with an inoculant addition of 0.4 %, and for inoculant B the surface component decreases even more. For both inoculant quantities the influence of wall thickness is shown. The lowest wall thickness has the highest surface component,

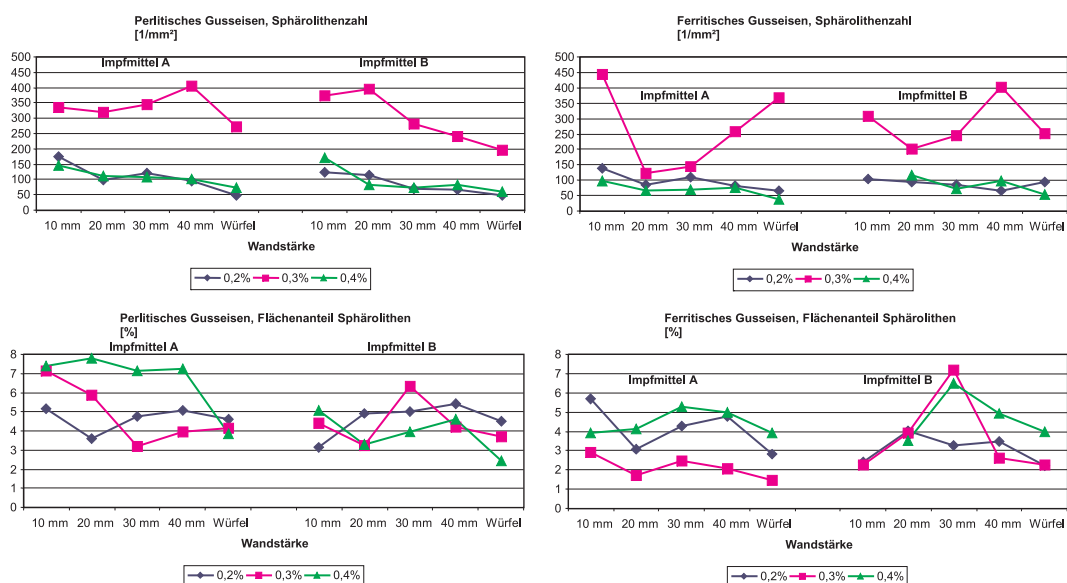


Figure 22. Graphite formation at test castings in plate design.



which equally lowers down above 30 mm up to 50 mm.

On ferritic cast iron the relation within wall thicknesses are not as unequivocally as at pearlitic cast iron, and the wall thickness of 30 mm seems to have a special position. The effect of inoculant A and B clearly differs on pearlitic and ferritic cast iron.

It has been shown that the thermal diffusivity as a value for cooling of a casting is very different within the different foundries, and by that it has to be clearly defined at each foundry as a decisive value for the solidification simulation. Variations of more than 30 % between the values of the different foundries are the rule.

At the tests for definition of the influence of different variable material values to the graphite precipitation in form of:

- number of spheroids,
- graphite quantity.

It has been shown that these values cannot alone give sufficient information about the quantity of eutectic graphite and by that about volume deficits or a shrinkage volume to be expected at solidification.

To be able to predict shrinkage volume by means of:

- physical values which define the solidification process,
- variable mould material values which define the solidification process,
- variable material values which define the solidification process.

It is necessary to get – on the side of material – one or more new quantitative parameter, which have to result from thermodynamic criterions of solidification.

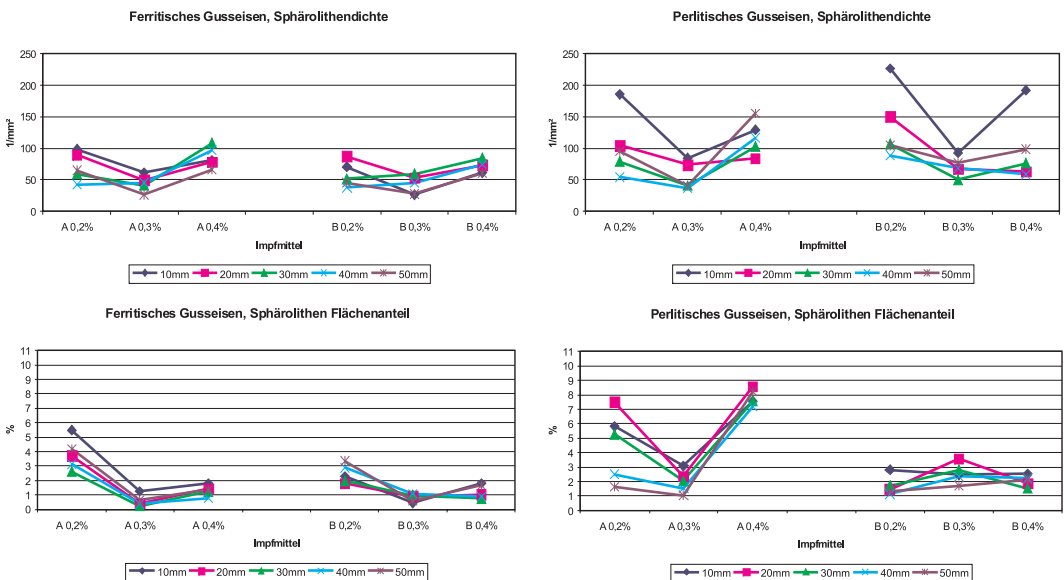


Figure 23. Graphite formation on casting of stepped wedges.

## PART 4: INFLUENCE OF MOULD AND MOULD MATERIAL

Besides the metal wall movement (Part 2) the mould wall movement (the attributes of the mould) is the second main influence factor that has an effect on “apparent shrinkage”. The dependence of the mould wall movement results of:

- type of mould material,
- composition of mould material,
- compaction,
- mould box attributes.

### Influence of mould box attributes

Four test cubes were positioned on a square pattern plate, each two of them with a modulus of 1.7 and 1.6 (Fig. 24). Each cube was equipped with the corresponding exothermic feeder.

By using this pattern equipment there were formed and cast three moulds, under simulation of different mould box attributes.

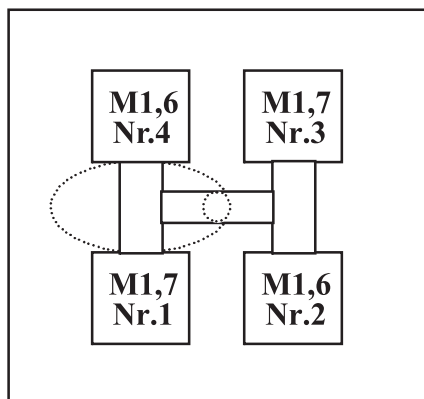


**Figure 24.** Construction of pattern plate

All the moulds were made of a clay bonded mould material (sand F32, 8 % bentonite A and ~ 2 % water) and compacted with a pneumatic



a) Without mould box



b) Filled in with resin bonded mould material



c) With mould box and charged

**Figure 25.** Simulation of mould box attributes

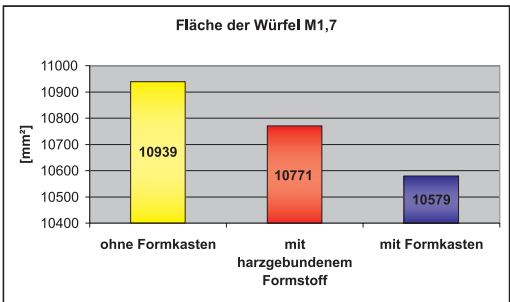
hand rammer. There was used spheroidal graphite cast iron  $S_R = 1$  as casting material:

- The first mould was poured **without mould box** (Fig. 25a). There was used a conical wooden frame during ramming. The frame was removed after compaction of the mould.
- The second mould was compacted by means of wooden frame, too. After removing this wooden frame there was set a metal frame around the mould. To increase the stability of the mould **resin bonded mould material was filled in between mould and metal frame** (Fig. 25b).
- To achieve an even higher mould stability it was chosen a rigid mould box for the third mould and the mould was charged (Fig. 25c).

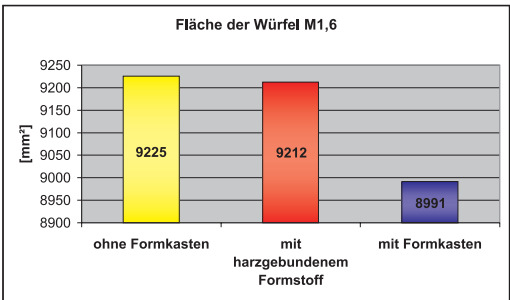
There were taken photos from the castings with sprue, runner and feeder as well as from the actual cubes. The mass of feeders and castings (cubes) were graphically evaluated, just as the surface of the cubes, sawed through the midst.

The evaluation of the surfaces should document the size of the enlargement of the three different moulds. For the purpose of comparison the contours of the sawed cubes were copied on a sheet of paper, scanned into the computer and calculated. The surfaces shown above were defined by means of the average values of the two indentic cubes of a mould.

Figure 26 shows the changes of the sawed cube surfaces for the three cast moulds in dependence of the “mould box stability”. The surfaces decrease on increasing stability of the mould, and there is to remark no difference within their behaviour between both moduli.

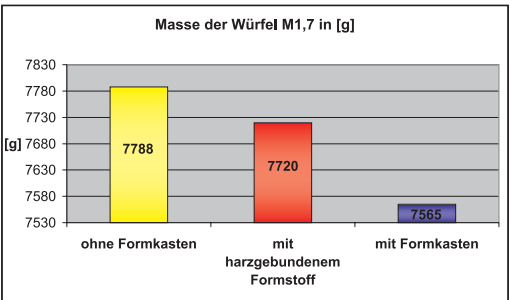


Surface of cubes M1,7

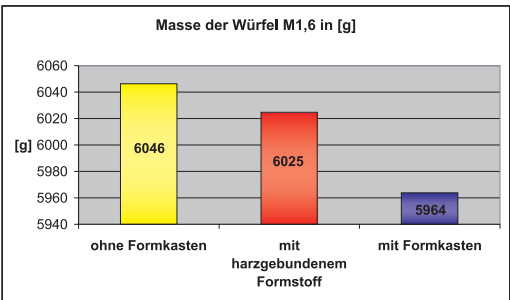


Surface of cubes M1,6

**Figure 26.** Surface of the cubes (M1,6 and M1,7)



Mass of cubes M1,7 (g)



Mass of cubes M1,6 (g)

**Figure 27.** Mass of the cubes (M1,6 and M1,7)

By evaluating the mass of cubes and feeders there should also be defined the size of the enlargement of the three moulds. For the purpose of comparison the feeders were sawed off, and feeders and cubes were separately weighed.

Figure 27 shows the mass of the cubes (M1.6 and 1.7) and Figure 28 shows the total masses (M1.6 and 1.7) of the three cast moulds. Just like the evaluation of the surfaces the masses shown in the figures were defined by means of the average values of the two identic cubes of a mould. On the X-axis there are shown the three moulds with the different box

attributes, on the Y-axis there are shown the masses (g).

The mass of the cubes decreases on increasing stability of the mould, and there is to remark no difference within their behaviour between both moduli.

The evaluation of the mass of cubes clearly shows, that the mass of the cube or the enlargement of mould is the smallest one by using a rigid mould box. The difference of enlargement is much less between the moulds without any mould box and the one with resin bonded mould material filled in between mould and metal frame.

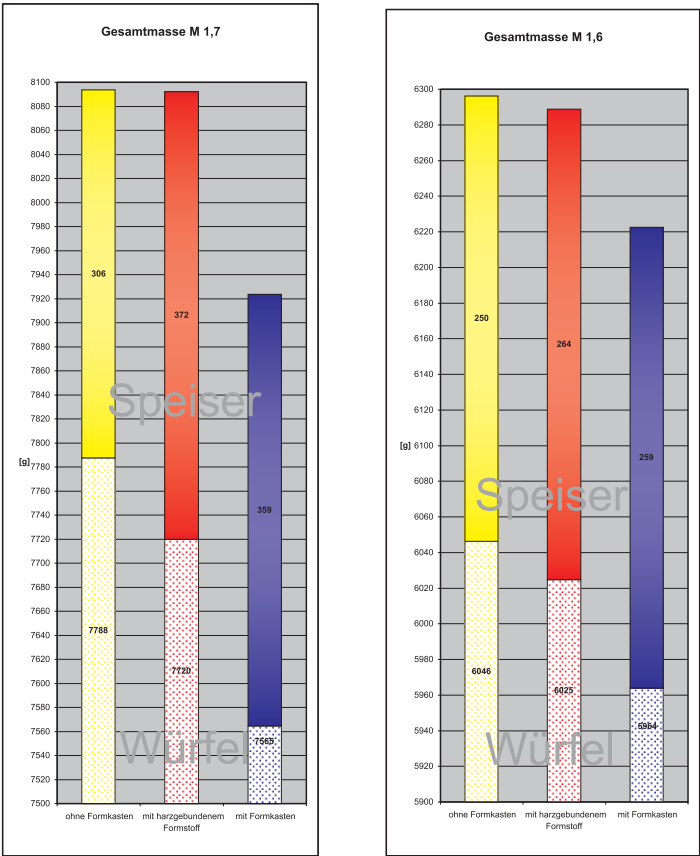


Figure 28. Mass of the cubes and feeders

First of all, you would assume that the cast quantity of iron or the total mass is identical for all the three moulds. But the representation of total mass (Fig. 28) shows that the mould enlarges already while pouring the cast iron into the mould. In this connection it becomes clear, that the enlargement is the smallest one by using a rigid mould box.

This test makes clear that the mould box attributes have influence on the mould wall movement. By comparing the differences between the masses extending of mould wall movement it is obviously mould wall movement can unequivocally define the feeding behaviour or the quality of a casting. The mould box attributes tested in this experiment are relative easy to stabilize in practice or should always be constant on a plant.

### The influence of type of bentonite / type of mould material

The pattern equipment or the arrangement of the cubes and the pouring system of the preceding tests have been taken over, and the cubes and the pouring system have been fixed

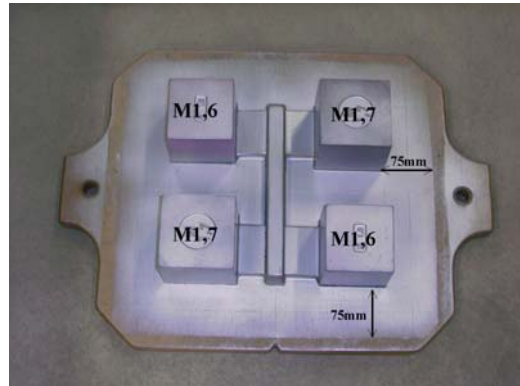


Figure 29. Pattern equipment

on a pattern plate, which could be installed in a moulding machine. As the distance of the cubes to the box border is important for the valuation of the influence of the mould wall movement, this distance has been the same at each cube (75 mm) (Fig. 29).

Three different types of bentonite were used. The relevant mould material attributes were measured and stated for each mixture, but they are not shown in this short version. There were produced four moulds with different contents of bentonite (5, 7, 9, 11 %) from each type of bentonite. There was added coal dust to each mould material

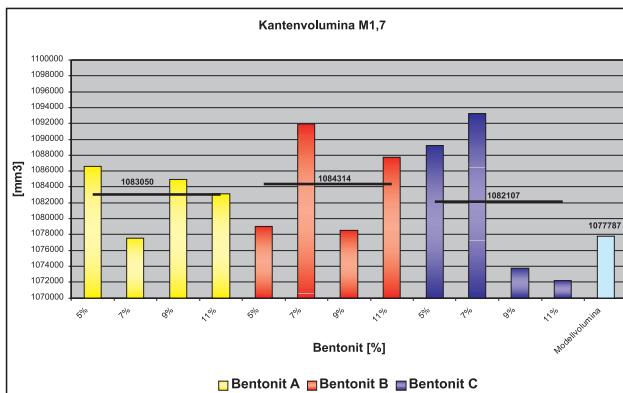


Figure 30. Edge volumes

mixture, the quantity was half of bentonites's content.

Just like the preceding tests silica sand F32 was prepared with the different bentonite types in a turbo-mixer. The cast iron ( $S_R = 1$ ) was melted in a medium frequency coreless crucible induction furnace.

In opposite to the preceding tests the cubes were not sawed and their surfaces were not evaluated, but the cube-edges were measured and the volume was calculated.

The evaluation of the edge-volume (Fig. 30) shows that for the three types of bentonite the average values of volume of the cast cubes was bigger than those of the original pattern volume, whereby there was no large difference between the three average values of edge-volume.

It can be assumed that the enlargement of a mould is not only defined by bulge of surfaces, but also by the enlargement of the "edge-frame" of the mould.

### Influence of the type of bentonite

The influence of the type of bentonite to the enlargement of the mould cavity is clearly to recognize in the evaluation of the mass of cubes (Fig. 31). The enlargement of mould cavity is the biggest one at type A and the smallest one at type C, whereby the difference of enlargement of mould cavity is not as large between bentonite type B and C as to bentonite type A.

The unequal behaviour of the three types of bentonite (Fig. 31) is hardly to interpret by means of the methylene blue value, as a comparison of these values is only possible for clay-types of the same origin. To give reasons for this behaviour an exact analysis of the attributes of the three bentonite-types would be necessary.

### Influence of bentonite content

The influence of the bentonite content to the enlargement of mould cavity is not easy to interpret for the three tests (Fig. 31-33).

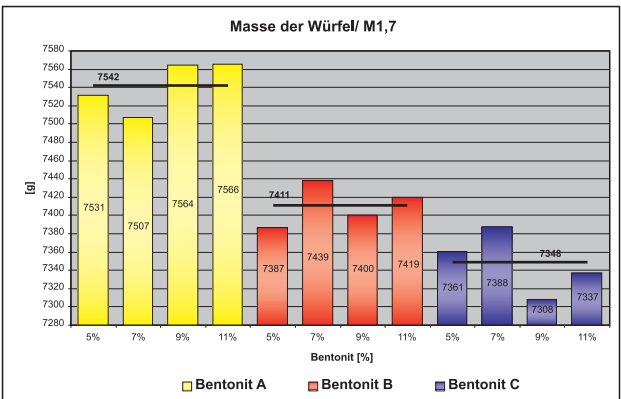


Figure 31. Masses of cubes with M 1.7



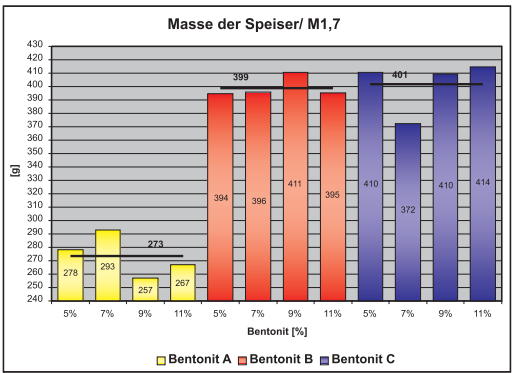


Figure 32. Masses of feeders

An important influence of the bentonite content to the enlargement of the mould cavity is not recognizable at the three cast tests.

But it has to be considered that the mechanical properties increase, too, with increasing bentonite content. But on all cast tests this overservation could not be connected with the enlargement of mould cavity.

To achieve the respective mould condition of each mixture at different bentonite contents each of the mould material mixtures need a different quantity of water. This

observation is easy to recognize, too, within the mould material analysis, and it directs to the fact that – besides the influence of the type of bentonite – the compactability (water content) seems to be the determining parameter for the size of the mould wall movement.

### “Apparent shrinkage”

The graphic evaluation of the total masses (Fig. 33) and the mass of the feeders (Fig. 32) shows that already while pouring, the moulds enlarge in different ways due to the ferrostatic pressure and the casting heat. Dependent bentonite-type the mass of the mould of bentonite-type C is a little smaller than those of bentonite-types A and B.

The enlargement of mould cavity and – as a consequence – an increase of cube mass is mainly marked at bentonite-type A. Here it flows the most material from feeder for compensation of mould space enlargement, whereby at type of bentonite B at approx. same total mass (Fig. 33) the mass of the cubes are clearly less, but therefore the mass

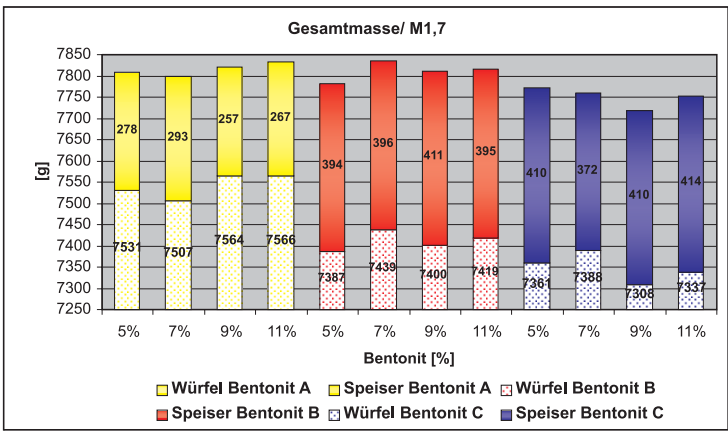


Figure 33. Total mass and partition to feeder and cube.

of the feeders are clearly larger than it is at bentonite type A. The mould space enlargement was smaller at this type of bentonite B with the consequence that less material from feeder was necessary for compensation of mould space enlargement. At same type of feeder bentonite B has a greater security against “apparent shrinkage”.

The enlargement of mould cavity at each type of bentonite does not show any tendency on change of bentonite contents.

As the influence of bentonite contents to the mould wall movement is not so important, it was taken an average value of eight cubes (M1.7) of each type of bentonites, which were produced with different contents of bentonite. At same time it was taken an average value of the corresponding eight compactabilities measured of the mould sand

mixtures. Figure 34 shows the average value of the mass of the cubes (M1.7) for each type of bentonite above the average value of the compactabilities.

The influence of the type of bentonite to the enlargement of mould cavity is clearly to see by means on Figure 34. By comparing the mass of cubes of the bentonite-types B and C the difference of masses is more than 60 g. Between type A and C there is even a difference of nearly 200 g. This is approx. 3 % of the cube-volume, this value could absolutely define the quality of a casting.

As a consequence of this test it becomes clear, that the type of bentonite and the compactability (water content) are two important parameters that define the enlargement of mould cavity and thereby define the “apparent shrinkage”.

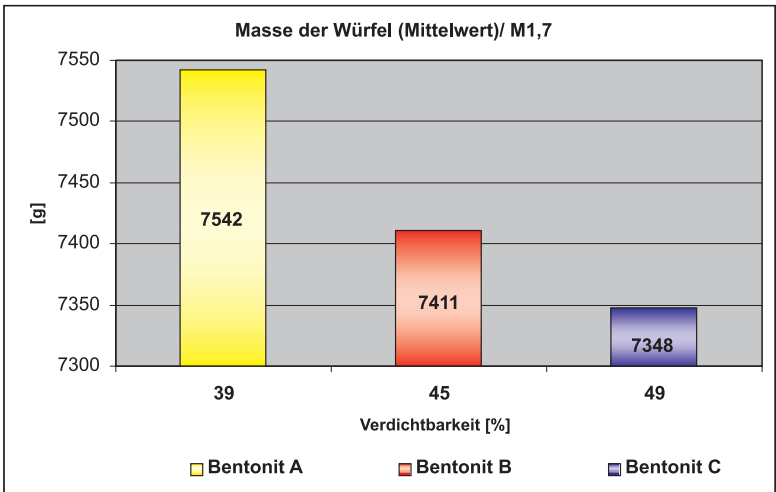


**Figure 34.** Average values of mass of cubes as function of average values of compactabilities of moulds

## SUMMARY

At first several physical values defining the solidification process are collected. These physical values are characterised as variable moulding material values after that.

Material values defining the solidification process are afterwards described and than their influence on feeding behaviour by chemical composition explained. The real feeding demand of a casting is described by influence of the mould and than the idea of

the “apparent shrinkage” is explained. With thermal analysis results an assessment tool for quality and solidification structure of cast iron. Feeding behaviour of a melt can be specified by this method.

Feeding is a transport phenomenon and there are several different feeding mechanisms during solidification time. It is shown that feeders are only active till 20 – 30 % of the solidification time.

This report will be continued.

## REFERENCES

- KOPPE, W.; ENGLER, S. (1962): *Giesserei* 49, Nr. 10/11, S. pp. 265-306.
- ENGLER, S.; DETTE, M. (1974): *Giesserei* 61, Nr. 26, S. pp. 769-774.
- ENGLER, S.; WOJTAS, H. J. (1979): *Giessereiforschung* 31, Nr. 1, S. pp. 37-44.
- FEICHTINGER, H. K. (1980): VSE-Tagung 22.01.1980 „Methoden der Qualitätsprüfung von Grauguss-Schmelzen“ (Institut für Metallurgie der ETH Zürich).